Isospin character of transitions to bound states in ^{204,206,208}Pb using inelastic scattering of ^{17}O ions

D. J. Horen, R. L. Auble, J. R. Beene, F. E. Bertrand, M. L. Halbert, G. R. Satchler, M. Thoennessen,* and R. L. Varner
Oak Ridge National Laboratory, Oak Ridge, Tennessee 37831

V. R. Brown and P. L. Anthony†
Lawrence Livermore National Laboratory, University of California, Livermore, California 94550

V. A. Madsen
Physics Department, Oregon State University, Corvallis, Oregon 97331
(Received 4 March 1991)

We have measured the scattering of 375-MeV ^{17}O ions by isotopes of ^{204,206,208}Pb to investigate the isospin character of transitions to low-lying 2^+ and 3^- states. The data were analyzed using the deformed optical potential model. The 2^+ collective strength, which is concentrated in a single state at 4.085 MeV in ^{208}Pb, is observed to fragment in both ^{204}Pb and ^{206}Pb. The differential cross sections for excitation of the collective 2^+ and 3^- states are well reproduced by model calculations in which it is assumed that $M_n/M_p = N/Z$ (i.e., isoscalar character). Angular distributions for the lowest-lying 2^+ states in ^{203,206}Pb are significantly different from those for the higher-lying collective 2^+ states, and can be reproduced with $M_n/M_p \approx 2.5$. The data are compared with random-phase-approximation calculations including pairing, and good agreement is found within estimated uncertainties.

I. INTRODUCTION

A controversy pertaining to the isospin character of the giant quadrupole resonance (GQR) located at an excitation energy of $E \sim 63 A^{-1/3}$ has existed for nearly a decade. Originally, it was believed that this resonance corresponded to the high-frequency isoscalar quadrupole mode predicted by Bohr and Mottelson [1]. However, the results from a series of papers on measurements of inelastic scattering of π^+/π^- suggested a strong isovector admixture in the GQR [2–6]. Nuclear structure calculations using random-phase approximation (RPA) indicate that the excitation of the GQR is mainly isoscalar with the ratio of neutron to proton multipole matrix elements given by $M_n/M_p \approx N/Z$ [7–9]. (Here, $M^L_{n,p} = \int \rho_{\rm tr}(r) r^{L+2} dr$ and we drop the L superscript.) Microscopic distorted-wave impulse-approximation (DWIA) calculations [7,9] of the pion cross sections using RPA wave functions result in ratios $R = \sigma(\pi^-)/\sigma(\pi^+)$ which are smaller than the experimental values for ^{118}Sn and ^{208}Pb. The difference between the calculated and experimental values is attributed in both cases to calculated $\sigma(\pi^+)$, which are considerably larger than the corresponding measured quantities. It should be noted that Auerbach, Klein, and Siciliano used continuum wave functions in their RPA calculation [7]. Although Brown, Carr, Madsen, and Petrovich [9] did not use continuum wave functions, they repeated the cross-section calculations using a neutron radius 10% larger than that for the protons in their comparison with the ^{118}Sn data. Even though the calculated $\sigma(\pi^+)$ are smaller than those obtained for the smaller ratio of neutron to proton radii, they are still about twice as large as the corresponding data for the GQR [9]. These authors concluded that the problem does not appear to be associated with differences in the neutron and proton transition densities in or beyond the nuclear surface. This is consistent with results from other microscopic calculations [7]. Modifications to the pion-nucleus interaction were also examined by Auerbach, Klein, and Siciliano [7] and shown to have a small effect on R.

The question becomes even more clouded when other pertinent work is considered. For example, Peterson and co-workers [10,11] have raised just this issue, i.e., since the excitation of the GQR lies in the unbound region, the neutron wave functions extend beyond those for the protons resulting in neutron transition densities that are larger than proton transition densities in the region of interaction for strongly absorbed projectiles such as pions. Microscopic DWIA calculations [11] using RPA wave functions produced $\sigma(\pi^-)$ in agreement with the data, but $\sigma(\pi^+)$ were again somewhat overestimated. In spite of the fact that all of the microscopic calculations conclude that there is a problem with the $\sigma(\pi^+)$ calculations (or data), the argument persists that the reported ratios of $\sigma(\pi^-)/\sigma(\pi^+)$ for excitation of states in the continuum are a reflection of the radial differences of the neutron and proton transition densities. In fact, Oakley *et al.* [12] have purported to demonstrate this effect by π^+/π^- measurements on a series of nickel isotopes, ^{58,60,62,64}Ni, where the neutron separation energies vary from 12.2 to 9.66 MeV. Using Tassie model transition densities in DWIA calculations, they deduce M_n/M_p ratios which increase from $\sim N/Z$ for ^{58,60}Ni to $\sim 1.54N/Z$ and $1.74N/Z$ for ^{62}Ni and ^{64}Ni, respectively. They argue that this variation of deduced M_n/M_p is a reflection of the

fact that use of Tassie transition densities does not properly reflect the radial differences of the neutron and proton transition densities imposed by the differences in neutron binding energies in this series of iostopes. Castel and co-workers [13–15] have used a similar argument and claim that although RPA calculations indicate that excitation of the GQR is nearly pure isoscalar, the pion interaction probes the nucleus only at densities significantly below $\frac{1}{8}$ of the central density. They then argue that the π^-/π^+ inelastic cross-section ratio is related to the ratio of the integrals of the neutron and proton transition matrix elements starting from an effective cutoff radius R_c rather than the origin. Since their RPA calculations indicate that the neutron transition densities extend beyond those for protons, they find effective ratios of M_n/M_p comparable to those deduced from analyses of π^-/π^+ measurements. However, as noted above, the DWIA calculations have shown this argument to be incorrect.

Recently, use has been made of the inelastic scattering of oxygen ions [16–18] and the deformed potential model [19] to deduce M_n/M_p using a single probe where both Coulomb and hadronic interactions are important. This method makes use of the interference between the nuclear and Coulomb amplitudes for excitation of the target state. The M_n/M_p deduced for ^{208}Pb [16,17] and ^{118}Sn [18] are in excellent agreement with the values expected for a pure isoscalar transition to the GQR. Furthermore, the M_p value deduced from an $(e,e'n)$ measurement [20] on ^{208}Pb also agrees well with the heavy-ion results. However, the M_p value deduced from a similar $(e,e'n)$ measurement [21] on ^{116}Sn is in better agreement with π^-/π^+ inelastic scattering than with that for oxygen on ^{118}Sn.

As has been noted in a previous work [18], if the correct interpretation of the π^-/π^+ data really did amount to determining a proper pion-nucleus interaction which samples the transition densities beyond some cutoff radius, then for consistency one would be forced to pose the same question as regards the heavy-ion data. In an attempt to get a better understanding of the relation between the pion and heavy-ion reactions, we obtained data for some bound states in ^{204,206,208}Pb well inside the grazing angle to provide a more stringent test of the deformed potential model analysis. We present data and analyses for excitation of the collective 2^+ and 3^- states in these nuclei, as well as the lowest-lying 2^+ levels (for which the transitions are not expected to be pure isoscalar) in ^{204,206}Pb. The latter could provide a critical comparison between the pion and heavy-ion methods.

II. EXPERIMENTAL

Measurements of the inelastic scattering of 375-MeV ^{17}O ions ($\sim$22 MeV/nucleon) by ^{204,206,208}Pb were made at the Holifield Heavy Ion Research Facility (HHIRF) using coupled operation of the 25-MeV Tandem Accelerator and the Oak Ridge Isochronous Cyclotron. The targets consisted of self-supporting foils of 0.50 mg/cm^2 areal density. The ^{206,208}Pb targets were enriched to $>99.6\%$, whereas the ^{204}Pb contained 63.12% ^{204}Pb, 16.15% ^{206}Pb, 7.58% ^{207}Pb, and 13.15% ^{208}Pb.

The scattered ^{17}O ions were detected at the focal plane of an Elbek broad range magnetic spectrograph with a quadrupole singlet magnet. Particle identification and reconstruction of the trajectories were made possible by the use of a parallel-plate avalanche counter, vertical drift chamber, and a segmented ion chamber. An overall energy resolution of about 250 keV FWHM was achieved. The spectrograph accepts $\Delta\Theta \approx 4.0°$, and several angular settings were used to cover the laboratory angular range from 5.5° to 19.5°. Elastic and inelastic data were taken simultaneously. The estimated uncertainty in the scattering angle is about $\pm 0.1°$. In the analyses, the data were binned in 0.25° intervals.

A comparison of the spectra obtained at $\Theta_{lab} = 13°$ for the three targets is shown in Fig. 1. The inelastic spectra are dominated by states excited by transitions with low-angular-momentum transfer (i.e., $L \leq 3$). The collective 3^- states which occur at 2.6 MeV in each isotope are strongly excited. The collective 2^+ strength, which is concentrated in a single state at 4.085 MeV in ^{208}Pb, is slightly fragmented (within our experimental resolution) in ^{206}Pb with most of the strength in a peak located at 4.107 MeV, and is even more strongly fragmented in ^{204}Pb. The peak in the ^{208}Pb spectrum just below 1 MeV arises from excitation of the 0.871-MeV, $\frac{1}{2}^+$ state in ^{17}O. In the ^{204,206}Pb spectra, contributions from this projectile excitation are mixed with those corresponding to excitation of the lowest-lying 2^+ states at 0.899 and 0.803 MeV, respectively.

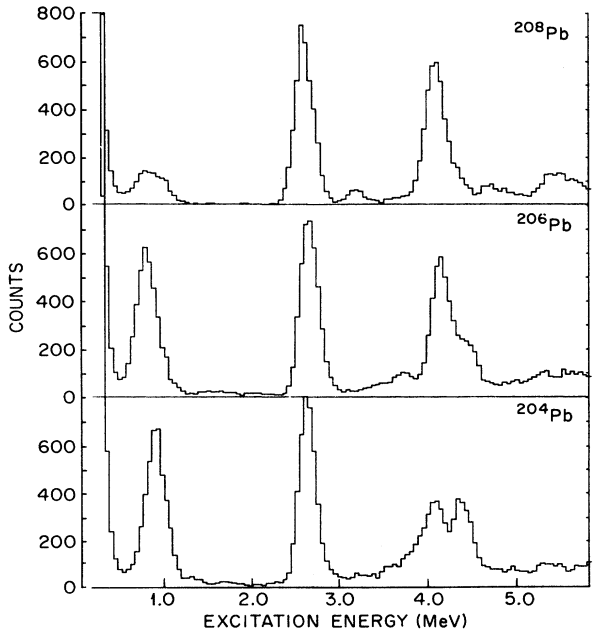

FIG. 1. Comparison of ^{204,206,208}Pb (^{17}O,^{17}O′) spectra obtained at $\Theta_{lab} = 13°$. The peak near 0.9 MeV in the ^{208}Pb spectrum arises from excitation of the 0.871-MeV, $\frac{1}{2}^+$ state of the ^{17}O projectile and its contribution must be subtracted from the ^{204,206}Pb spectra (see text).

III. DATA ANALYSIS AND DISCUSSION

A. Elastic scattering

The angular distributions for elastic scattering from the three targets are essentially identical. In Fig. 2, we show the results of an optical-model search using the computer program PTOLEMY [22] compared with the elastic-scattering data for ^{208}Pb. The optical-model potential was assumed to be of the Woods-Saxon form

$$U(r)=-Vf(x_V)=iWf(x_W)\ ,$$

with

$$f(x_i)=(1+e^{x_i})^{-1},\quad x_i=(r-R_i)/a_i\ ,$$

$$R_i=r_i(A_p^{1/3}+A_t^{1/3})\ ,$$

and $i=V,W$. The Coulomb potential was taken to be that of a point charge interacting with a uniform charge distribution with radius $R_c=r_c(A_p^{1/3}+A_t^{1/3})$ fm. Numerous searches were carried out in which a variety of combinations of the optical parameters were allowed to vary. The resulting fits to the data were comparable. We present in Fig. 2 the results obtained by fixing $V=40.0$ MeV, and searching on W, $r_V=r_W$, and $a_V=a_W$. The overall fit to the data (which involves no renormalization) is good. The deviations between the calculated curve and the data at angles $\Theta_{cm}<9°$ probably result from errors associated with reconstruction of the small-angle trajectories. The error bars noted on the figure include all uncertainties except those for the scattering angle. The optical-model parameters adopted for all the calculations shown in the figures are $V=40.0$ MeV, $W=42.499$ MeV, $r_V=r_W=1.1475$ fm, $a_V=a_W=0.7670$ fm, and $r_c=1.20$ fm.

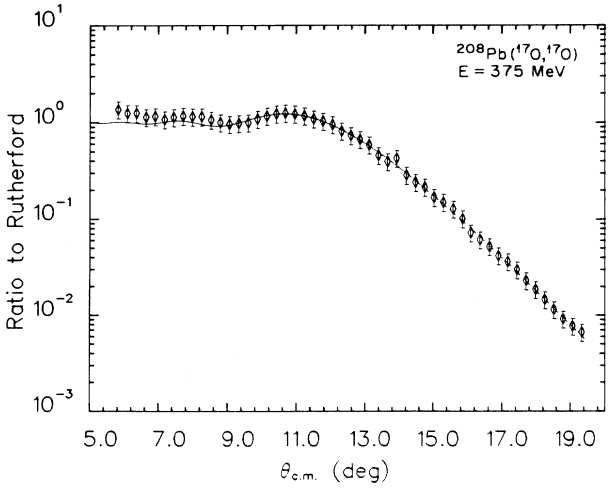

FIG. 2. Optical model fit to ^{208}Pb+^{17}O elastic-scattering data at $E=375$ MeV. The data are given in terms of the ratio to the Rutherford cross section. The parameters resulting from this fit are given in the text.

B. Inelastic scattering

Differential cross sections were determined for excitation of the 3^- and 2^+ collective states in ^{204,206,208}Pb and the first 2^+ states in ^{204,206}Pb. The 3^- states in ^{204,206}Pb are reported to lie at 2.618 and 2.647 MeV with $B(E3)\uparrow=0.66$ and 0.65 e^2b^3, respectively [23]. We find that the collective 2^+ strength near 4 MeV is ^{206}Pb can be decomposed into three fragments with relative strengths of 8% at 3.675 MeV, 69% at 4.107 MeV, and 23% at 4.413 MeV. The collective 2^+ strength in ^{204}Pb is comprised of four fragments. After correcting for the ^{206,207,208}Pb content in the ^{204}Pb target, we estimate the relative intensities of these to be 11% at 3.554 MeV, 22% at 3.804 MeV, 17% at 4.044 MeV, and 50% at 4.362 MeV. Within experimental uncertainties, all of the assigned collective 2^+ fragments have similar angular distributions. The total strength for this collective excitation is about the same in ^{204,206,208}Pb. The centroid of the distribution in ^{204}Pb is 4.100 MeV and in ^{206}Pb 4.140 MeV.

The differential cross sections for exciting the collec-

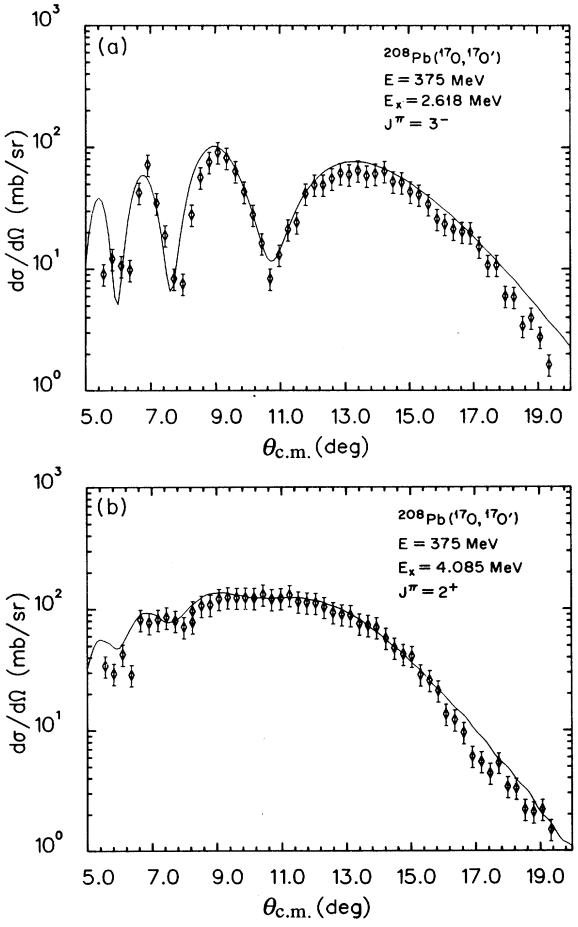

FIG. 3. Differential cross sections for excitation of the states at (a) 2.618 MeV (3^-) and (b) 4.085 MeV (2^+) in ^{208}Pb. The solid curves result from DWA calculations using optical model potential parameters determined from fitting the ^{208}Pb+^{17}O elastic data. In these calculations, $M_n/M_p=N/Z$.

tive 3^- and 2^+ states in ^{208}Pb at 2.618 and 4.085 MeV, respectively, are shown in Fig. 3. Differential cross sections for exciting the analogous strength in ^{204}Pb, i.e., 3^- state at 2.618 MeV and group of states near 4.1 MeV, are shown in Fig. 4. To determine the differential cross sections for excitations of the first 2^+ states in ^{204,206}Pb, the data have to be corrected for the $E2$ excitation of the first excited state (0.871 MeV, $\frac{1}{2}^+$) of the ^{17}O projectile. This was accomplished by normalizing the ^{208}Pb elastic data to that of ^{204,206}Pb for each angle bin, and subtracting the ^{17}O* peak in the ^{208}Pb spectrum. Angular distributions for exciting the first 2^+ states in ^{204,206}Pb are shown in Fig. 5. The error bars shown on the data represent our estimate of all contributions to the uncertainties.

The deformed potential model [19] was used with the program PTOLEMY [22] in both the distorted-wave approximation (DWA) and the exact coupled-channels solution. The effects on the elastic-scattering cross sections predicted by the latter method were negligible, thereby indicating that the effects of coupling to the elastic channel are unimportant. The curves presented in the figures were obtained from coupled-channels calculations.

Nuclear transition potentials for angular momentum transfer L are assumed [19] as

$$H_L^N(r) = -\delta_V(L)\frac{dV(r)}{dr} - i\delta_W(L)\frac{dW(r)}{dr} ,$$

where $V(r)$ and $W(r)$ are taken from fits to the elastic data. In this work, the real and imaginary deformation lengths are assumed equal [i.e., $\delta_V(L)=\delta_W(L)=\delta_L$]. The Coulomb interaction is represented in the form of a multipole expansion between a point charge and a uniformly charged sphere with radius R_c, i.e.,

$$H_L^c(r) = \frac{4\pi Z_p e}{2L+1}[B(EL)\uparrow]^{1/2} \times \begin{cases} r^L/R_c^{2L+1}, & r < R_c, \\ 1/r^{L+1}, & r \geq R_c, \end{cases}$$

where Z_p is the atomic number of the projectile and $B(EL)\uparrow$ is the charge multipole moment. The model [19] assumes that the deformation length of the transition potential is equal to that of the nuclear density distribution.

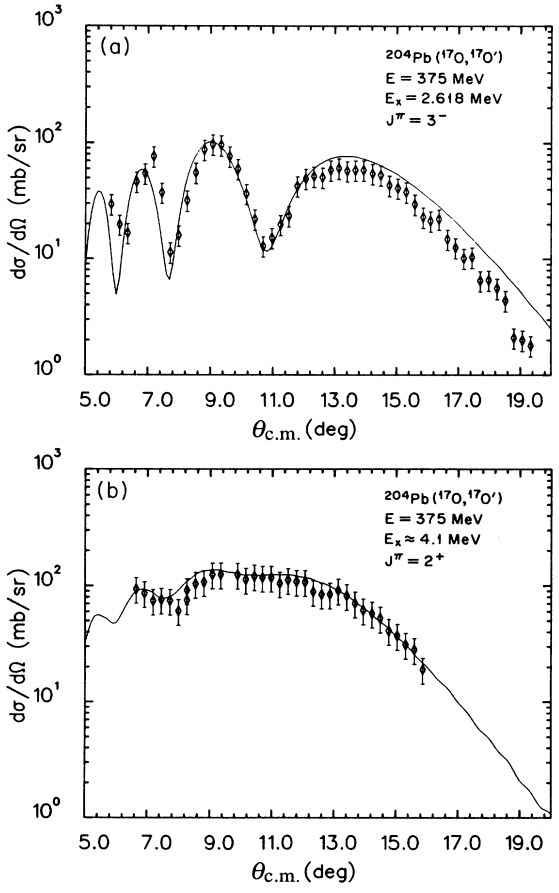

FIG. 4. Differential cross sections for (a) the 3^- (2.618 MeV) and (b) 2^+ (~4.1 MeV) collective excitations in ^{204}Pb.

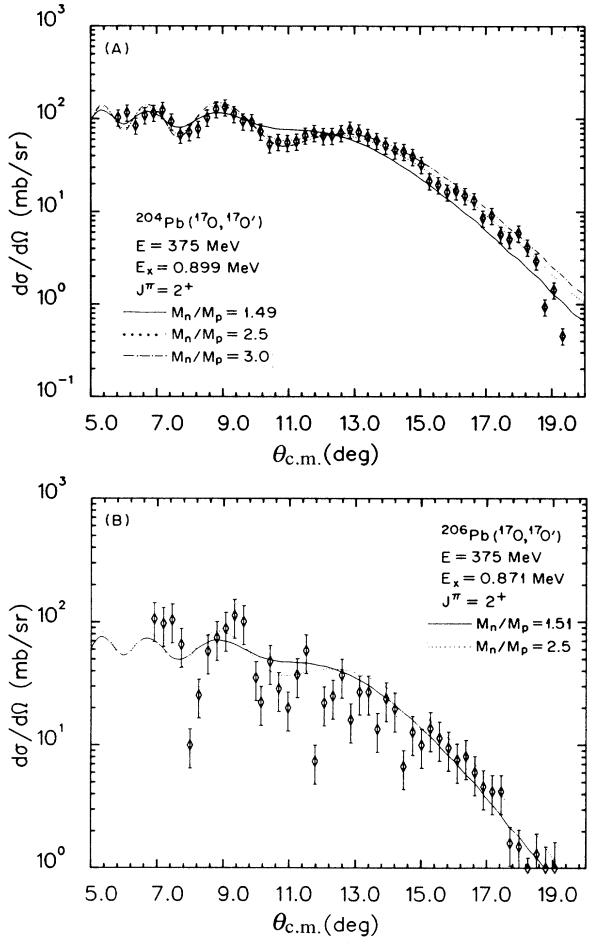

FIG. 5. Differential cross sections for excitation of the lowest-lying 2^+ states at (a) 0.899 MeV in ^{204}Pb and (b) 0.803 MeV in ^{206}Pb. The value of M_n/M_p used for each curve shown is indicated on the figure.

The mass multipole moment can then be expressed as

$$B(L)\uparrow=\delta_L^2\left[\frac{3A}{4\pi}R^{L-1}\right]^2$$

if a uniform distribution with radius R is assumed [19]. One can also write the mass multipole moment in terms of the r^L radial moments of the neutron and proton transition densities; i.e.,

$$B(L)\uparrow=|M_n+M_p|^2 .$$

Since $B(EL)\uparrow=|M_p|^2$, one finds

$$\left|\frac{M_n}{M_p}\right|=\left[\frac{B(L)\uparrow}{B(EL)\uparrow}\right]^{1/2}-1 ,$$

which is an indication of the isospin character for the excitation. For multipoles with $L\geq 2$, the deformation length δ_L corresponding to 100% of the isoscalar energy-weighted sum rule (EWSR) is given by the relation

$$\delta_L^2=2\pi\hbar^2\frac{L(2L+1)}{3mAE_x} ,$$

where m is the nucleon mass, A is the mass number, and all of the strength is assumed to be localized at an excitation energy E_x.

The magnitude and shape of the differential cross section are dependent upon the magnitudes of the nuclear and Coulomb amplitudes as well as their relative phase. In principle, one can determine two quantities by comparing the calculations with the data, e.g., δ_L (or M_n/M_p) and $B(EL)\uparrow$. In our analyses, we fix the value of $B(EL)\uparrow$ when it is known from other work.

C. Discussion

Collective excitations. The differential cross section for exciting the collective 3^- state at 2.618 MeV in ^{208}Pb was calculated using the adopted [23] $B(E3)\uparrow=0.611\ e^2b^3$ and $M_n/M_p=N/Z$ (i.e., pure isoscalar). It is clear from Fig. 3(a) that the deformed potential model does an excellent job of reproducing both the magnitude and shape of the experimental data. For the collective 2^+ state at 4.085 MeV in ^{208}Pb, we use the adopted [24] $B(E2)\uparrow=0.290\ e^2b^2$ and $M_n/M_p=N/Z$. Again, one finds that the calculated curve [see Fig. 3(b)] is in excellent agreement with the data. We believe that the deviations at the smallest angles are primarily experimental. Calculations for these two collective levels were also performed, including reorientation coupling in order to investigate its effect on the differential cross sections. In these calculations, we assumed a rotor-model coupling scheme and the same nuclear transition potential for both the excitation and reorientation interactions. This model implies static quadrupole moments for the excited states which are several times the measured [25] values. The differences between the calculations with and without reorientation were found to be negligible.

Our cross section for excitation of the 3^- state at 2.647 MeV in ^{206}Pb is equal to that for excitation of the analogous level in ^{208}Pb within experimental uncertainties. This suggests that the $B(E3)\uparrow$ for ^{206}Pb is equal to that for ^{208}Pb, which agrees with the unpublished (e,e') results of Papanicolas [26]. The cross section for exciting the peak at 2.6 MeV in the ^{204}Pb target is nearly identical to that obtained for ^{208}Pb. The cross section for the ^{204}Pb target can be expressed in terms of the isotopic compositions, the ^{204}Pb and ^{208}Pb cross sections, and the ratio of the ^{206,207}Pb cross sections to that of ^{208}Pb. As noted the ^{206}Pb to ^{208}Pb ratio is 1.0, which is about 6% lower than would be expected from the tabulated [23] $B(E3)\uparrow$. Papanicolas [26] also reports a ratio of 1.0 for the ^{207}Pb to ^{208}Pb cross sections, which is about 15% larger than would be expected assuming the cross sections are proportional to the $B(E3)\uparrow$ values [27]. For our analysis, we adopt a value of 1.0 for these cross-section ratios, which then indicates that the cross section for exciting the collective 3^- state at 2.618 MeV in ^{204}Pb is the same as the cross section for the 2.6-MeV peak of the ^{204}Pb target. This cross section, which is nearly identical to that for the 3^- state in ^{208}Pb, is shown in Fig. 4(a). The curve in Fig. 4(a) was calculated using $B(E3)\uparrow=0.611\ e^2b^3$ (the same as for ^{208}Pb).

As noted earlier, the collective 2^+ excitations in ^{204,206}Pb are fragmented relative to that in ^{208}Pb. The summed cross section for this collective excitation for the ^{204}Pb target is shown in Fig. 4(b). From a comparison of these data with those for the 4.085-MeV level of ^{208}Pb shown in Fig. 3(b), one can see that the two data sets are almost identical in magnitude as well as in shape. The summed cross section near the grazing angle for this excitation in ^{206}Pb is the same as that for ^{208}Pb. Hence, the summed $B(E2)\uparrow$ for this excitation in ^{206}Pb is similar to that for ^{208}Pb. This information was used with the known data [26,27] for this collective excitation in ^{207}Pb to deduce the relative strength distribution in ^{204}Pb noted earlier. The calculated curve corresponding to the collective 2^+ excitation in ^{204}Pb used the same $B(E2)\uparrow=0.290\ e^2b^2$ as for ^{206,208}Pb.

First 2^+ states in ^{204,206}Pb. Cross sections corresponding to the peaks near 0.9 MeV in the ^{204,206}Pb targets (see Fig. 1) were determined after subtracting the contribution to the peak areas arising from excitation of the 0.871-MeV state of the projectile. For the ^{206}Pb target, the resulting cross section corresponds to that for excitation of the 0.803-MeV state, and this is shown in Fig. 5(b). To obtain the cross section for excitation of the 0.899-MeV state in ^{204}Pb, contributions due to the ^{206,207}Pb impurities in the ^{204}Pb target had to be subtracted. This was done by utilizing the isotopic composition of the ^{204}Pb target, and assuming that the relative contributions to the cross sections were proportional to the relative $B(E2)\uparrow$ for the states involved. The differential cross section for exciting the 0.899-MeV state in ^{204}Pb is shown in Fig. 5(a).

We calculate the cross sections for exciting the first 2^+ states in ^{204,206}Pb by taking the adopted [24] values of $B(E2)\uparrow=0.162$ and $0.100\ e^2b^2$, respectively, and using various choices of M_n/M_p. For the comparison with the ^{204}Pb data, we show three calculations, one for an isoscalar transition in which $M_n/M_p=N/Z$ $(=1.49)$ and the

others for $M_n/M_p=2.5$ and 3.0. It is clear from Fig. 5(a) that the isoscalar value grossly fails to reproduce the shape of the angular distribution. The larger values reproduce the magnitude of the maxima near 7° and 9°, and also the position of the maximum near the grazing angle (i.e., 13°) as well as the depth of the minimum near 10°. From the overall agreement with the data, it appears that $M_n/M_p \sim 2.5-3.0$ for this transition.

A similar comparison is made in Fig. 5(b) for the 0.803-MeV first 2^+ state in ^{206}Pb. Unfortunately, the data for ^{206}Pb have larger uncertainties than those for ^{204}Pb because of poorer statistics. Even so, the data indicate a depression in the cross section near 11°, which is a signature for $M_n/M_p > N/Z$. The dotted curve has been calculated with $M_n/M_p=2.5$.

RPA calculations. The calculations presented here, which have been described in detail elsewhere [9], utilize a quasiparticle RPA model with separable isoscalar and isovector particle-hole interactions. The present results for ^{208}Pb have been compared to other RPA calculations in Ref. [28], and are shown there as entry d of Table I. The same input parameters used here for the ^{208}Pb 2^+ and 3^- calculations, including the particle-hole interaction and single-particle energies, are also used for ^{204,206}Pb. The quasiparticle energies and pairing occupancy for the open neutron shells in ^{204}Pb and ^{206}Pb are calculated with the same pairing force. The pairing force gave a gap of 0.9 MeV for ^{204}Pb and 0.78 MeV for ^{206}Pb. A different pairing force producing relatively smaller gaps was also used to test the sensitivity; the results were qualitatively the same. The configuration space includes single-particle orbits $3\hbar\omega$ above and below the Fermi surface. Since we use a harmonic-oscillator basis with a separable multipole operator, this space includes all possible particle-hole contributions for the 3^- multipolarity and goes beyond what is needed for the 2^+.

TABLE I. Comparison between experimental $B(EL)\uparrow$ and M_n/M_p for 2^+ and 3^- bound states in ^{204,206,208}Pb and values calculated from an RPA code using a separable interaction and including pairing.

		Experiment			RPA calculation		
		E_x	$B(EL)\uparrow$		E_x	$B(EL)\uparrow$	
Isotope	J^π	(MeV)	(e^2b^{2L})	M_n/M_p	(MeV)	(e^2b^{2L})	M_n/M_p
208	3^-	2.618	0.611	1.54[a]	3.10	0.645	1.56
	2^+	4.085	0.290	1.54[a]	4.55	0.251	1.66
206	3^-	2.647	0.61	1.51[a]	3.36	0.618	1.50
	2^+	0.803	0.100	~2.5	1.57	0.0829	2.2
		3.675			3.65		
		4.107	0.29	1.51[a]	|	0.291	~1.68
		4.413			4.87		
204	3^-	2.618	0.61	1.49[a]	3.52	0.566	1.45
	2^+	0.899	0.162	~2.5	1.59	0.181	2.2
		3.554			3.43		
		3.804	0.29	1.49[a]	|	0.165	~1.8
		4.044			|		
		4.362			4.97		

[a]For these collective excitations, the data are well reproduced by using $M_n/M_p=N/Z$.

The calculated energies, $B(EL)\uparrow$, and M_n/M_p are compared with the experimental values in Table I. The overall agreement for the 2^+ and 3^- states in ^{208}Pb is seen to be quite good, although the calculated level energies are high by about 0.5 MeV. The calculated energies for the levels in ^{204,206}Pb are also high. This is a common problem in all the RPA calculations of Ref. [28] and in other similar calculations [29–31]. In the quasiparticle RPA model of Pomar, Blomqvist, Liotta, and Insolia [31], in which four-quasiparticle states were included, it was found that the first 2^+ state of ^{204}Pb could be reproduced by multiplying matrix elements involving the $1h_{9/2}$ and $2f_{7/2}$ shells by a factor of 1.95. The calculations of Gillet, Giraud, and Rho [32] provide a reasonable fit to the first 2^+ level energies, but predict $B(E2)$'s which are low by an order of magnitude.

Considering realistic uncertainties in both the experimental and calculated quantities, the agreement in the $B(E)\uparrow$ values for the 3^- levels in ^{204,206}Pb is good. Likewise, this is true for the $B(E2)\uparrow$ and M_n/M_p values for the first 2^+ states in ^{204,206}Pb. (Our model calculations of the $B(E2)\uparrow$ values for the first 2^+ states in ^{204,206}Pb are in better agreement with the data than similar type calculations [29–33] which have used more limited configuration space.) This would suggest that application of the deformed potential model is valid for these transitions.

In the doubly closed-shell nucleus ^{208}Pb, there are no $0\hbar\omega$ valence configurations. For 2^+ excitations, the valence space is comprised of four $1\hbar\omega$ type transitions, two for neutrons and two for protons. These configurations involve transitions from the spin-orbit intruders ($i_{13/2}$ for neutrons and $h_{11/2}$ for protons) to higher-lying orbits within their own harmonic-oscillator shell. All other 2^+ configurations involve at least $2\hbar\omega$, i.e., GQR-type excitations. The RPA low-lying collective-state solution arises as a result of the mixing of the two spaces in the diagonalization. In a schematic-model picture [34] this would be the core-polarization effect of the GQR on the first 2^+ state. For ^{208}Pb, the RPA mixing yields a first 2^+ state with $M_n/M_p \approx N/Z$. For the isotopes ^{204,206}Pb, in addition to the $1\hbar\omega$ configurations present in ^{208}Pb, there are neutrons in the $0\hbar\omega$ valence space. The first 2^+ states in these isotopes are the result of the mixing of the three spaces in the diagonalization. The expectation from the schematic mode [34] for single-closed-shell neutron-valence nuclei is that the first 2^+ state has M_n/M_p greater than N/Z. The results in Table I are consistent with this expectation.

There should also be collective states in ^{204,206}Pb at about the same energy and in analogy with the 2^+ state at 4.085 MeV in ^{208}Pb. The valence space is the same as the $1\hbar\omega$ valence space in ^{208}Pb; the difference is that now these configurations are not lowest in energy, hence, they will mix with the $2\hbar\omega$ states above and the pure neutron $0\hbar\omega$ states below in much the same way as the "reversal states" of Ref. [35]. From a schematic-model point of view, they will be core polarized from the GQR above, and in turn they will core polarize the first 2^+ state below. The isospin character of the transitions and the

excitation energies for the states resulting from the full RPA diagonalization are consistent with this expectation. In Table I it can be seen that there is not a single collective state in ^{204,206}Pb, but a band of states; this is caused by mixing with the $0\hbar\omega$ configurations which result from pairing. Although the inclusion of other effects, such as two-particle two-hole contributions, might alter these results, the sum-rule strength would be conserved. Consequently, the RPA results for the $B(E2)\uparrow$ and M_n/M_p for this band of states shown in Table I was obtained by concentrating their sum-rule strength at 4.1 MeV.

A feature not evident in Table I is that the transition isospin of the low-lying 2^+ states (as indicated by the magnitude of M_n/M_p) actually decreases smoothly with increasing excitation energy such that M_n/M_p drops from its maximum value for the first 2^+ state to a value around 1.6, slightly more than N/Z, at the top of the collective band. This is consistent with the transition isospin dependence expected from the point of view of the sharing of collective multipole strength in the nuclear particle-hole model in Ref. [36].

The observed and calculated $B(E2)\uparrow$ and M_n/M_p are in excellent agreement for the 2^+ collective state in ^{206}Pb. The disparity between these values for the ^{204}Pb comparison may not be quite as bad as indicated in Table I because the uncertainties in both the experimental and calculated quantities are considerably larger than for the case of ^{206}Pb.

IV. SUMMARY

We have made measurements of inelastic scattering of ^{17}O ions on ^{204,206,208}Pb and studied the excitation of bound 2^+ and 3^- states in these nuclei. It has been found that the differential cross sections can be well reproduced by DWA calculations using the deformed optical potential model transition densities. RPA calculations of the $B(EL)\uparrow$ and M_n/M_p for these transitions are in good agreement with the experimentally deduced quantities. In particular, this holds even for excitation of the lowest-lying 2^+ states in ^{204,206}Pb which involves a significant admixture of isospin. [These results are quite consistent with schematic-model expectations [34] for single-closed-shell neutron (proton-) valence nuclei, which predict M_n/M_p greater than (less than) N/Z, and with studies [37] that have deduced M_n/M_p by utilizing different probes.] This suggests that even for these cases, use of the deformed optical potential model in the analysis of data obtained with a single probe is a valuable tool in testing nuclear structure calculations of transition isospin. Of course, a full understanding of why the deformed optical potential model works so well for transitions of mixed isospin must still await detailed folding model calculations.

A comparison of the present results for the lowest-lying 2^+ states in ^{204,206}Pb with π^+/π^- inelastic scattering could prove instrumental in achieving an understanding of the problem noted in the introduction of this paper.

ACKNOWLEDGMENTS

This work was sponsored by the U.S. Department of Energy under Contract No. DE-AC05-84OR21400 with Martin Marietta Energy Systems, Inc., No. W-7405-ENG-48 at Lawrence Livermore National Laboratory, and No. DE-AT06-79ER-10405 at Oregon State University.

*Present address: Cyclotron Laboratory, Michigan State University, East Lansing, MI 48824.

†Present address: Fermi National Accelerator Laboratory, Batavia, IL 60510.

[1] A. Bohr and B. R. Mottelson, *Nuclear Structure* (Benjamin, New York, 1975), Vol. 2.

[2] J. L. Ullmann, J. J. Kraushaar, T. G. Masterson, R. J. Peterson, R. S. Raymond, R. A. Ristinen, N. S. P. King, R. L. Boudrie, C. L. Morris, W. W. True, R. E. Anderson, and E. R. Siciliano, Phys. Rev. Lett. **51**, 1038 (1983).

[3] C. L. Morris, S. J. Seestrom-Morris, and L. C. Bland, in Proceedings of the International Symposium on Highly Excited States and Nuclear Structure, Orsay, France, edited by N. Marty and N. Van Gai [J. Phys. (Paris) Colloq. **45**, C4-327 (1984)].

[4] J. L. Ullmann, J. J. Kraushaar, T. G. Masterson, R. J. Peterson, R. S. Raymond, R. A. Ristinen, N. S. P. King, R. L. Boudrie, C. L. Morris, R. E. Anderson, and E. R. Siciliano, Phys. Rev. C **31**, 177 (1985).

[5] S. J. Seestrom-Morris, C. L. Morris, J. M. Moss, T. A. Carey, D. Drake, J. C. Dousse, L. C. Bland, and G. S. Adams, Phys. Rev. C **33**, 1847 (1986).

[6] J. L. Ullmann, P. W. F. Alons, B. L. Clausen, J. J. Kraushaar, J. H. Mitchell, R. J. Peterson, R. A. Ristinen, R. L. Boudrie, N. S. P. King, C. L. Morris, J. N. Knudson, and E. F. Gibson, Phys. Rev. C **35**, 1099 (1987).

[7] N. Auerbach, Amir Klein, and E. R. Siciliano, Phys. Rev. C **31**, 682 (1985).

[8] J. Wambach, Phys. Rev. C **31**, 1950 (1985).

[9] V. R. Brown, J. A. Carr, V. A. Madsen, and F. Petrovich, Phys. Rev. C **37**, 1537 (1988).

[10] R. J. Peterson and J. L. Ullmann, Nucl. Phys. **A435**, 717 (1985).

[11] R. J. Peterson and R. de Haro, Nucl. Phys. **A459**, 445 (1986).

[12] D. S. Oakley, M. R. Braunstein, J. J. Kraushaar, R. A. Loveman, R. J. Peterson, D. J. Rilett, and R. L. Boudrie, Phys. Rev. C **40**, 859 (1989).

[13] P. M. Boucher and B. Castel, Z. Phys. **A334**, 381 (1989).

[14] B. Castel, P. M. Boucher, and H. Toki, J. Phys. G **15**, L237 (1989).

[15] B. Castel and H. Toki, Nucl. Phys. **A514**, 682 (1990).

[16] D. J. Horen, J. R. Beene, and F. E. Bertrand, Phys. Rev. C **37**, 888 (1988).

[17] J. R. Beene, F. E. Bertrand, D. J. Horen, R. L. Auble, B. L. Burks, J. Gomez del Campo, M. L. Halbert, R. O. Sayer, W. Mittig, Y. Schultz, J. Barrette, N. Alamanos, F. Auger, B. Fernandez, A. Gillibert, B. Haas, and J. P. Vivien, Phys. Rev. C **41**, 920 (1990).

[18] D. J. Horen, F. E. Bertrand, J. R. Beene, G. R. Satchler,

W. Mittig, A. C. C. Villari, Y. Schutz, Zhen Wenlong, E. Plagnol, and A. Gillibert, Phys. Rev. C **42**, 2412 (1990).
[19] G. R. Satchler, *Direct Nuclear Reactions* (Oxford University Press, Oxford, 1983); Nucl. Phys. **A472**, 215 (1987).
[20] G. O. Bolme, L. S. Cardman, R. Doerfler, L. J. Koester, Jr., B. L. Miller, C. N. Papanicolas, H. Rothaas, and S. E. Williamson, Phys. Rev. Lett. **61**, 1081 (1988).
[21] R. A. Miskimen, E. A. Ammons, J. D. T. Arruda-Neto, L. S. Cardman, P. L. Cole, J. R. Deininger, S. M. Dolfini, A. J. Linzey, J. B. Mandeville, B. L. Miller, P. E. Mueller, C. N. Papanicolas, A. Serdarevic, and S. E. Williamson, Phys. Lett. **236**, 251 (1990).
[22] M. H. Macfarlane and S. C. Pieper, Argonne National Laboratory Report No. ANL-76-11 (Rev. 1) 1978 (unpublished); M. Rhoades-Brown, M. H. Macfarlane, and S. C. Pieper, Phys. Rev. C **21**, 2417 (1980); **21**, 2436 (1980).
[23] R. H. Spear, At. Data Nucl. Data Tables **42**, 55 (1989).
[24] S. Raman, C. H. Malarkey, W. T. Milner, C. W. Nestor, Jr., and P. H. Stelson, At. Nucl. Data Tables **36**, 1 (1987).
[25] M. J. Martin, Nucl. Data Sheets **47**, 797 (1986).
[26] C. N. Papanicolas, Ph.D. thesis, Massachusetts Institute of Technology, 1979 (unpublished).
[27] M. R. Schmorak, Nucl. Data Sheets **43**, 383 (1984).
[28] E. L. Hjort, F. P. Brady, J. L. Romero, J. R. Drummond, M. A. Hamilton, B. McEachern, R. D. Smith, V. R. Brown, F. Petrovich, and V. A. Madsen, Phys. Rev. Lett. **62**, 870 (1989).
[29] M. Barranco, R. J. Lombard, and D. Mas, Phys. Lett. **91B**, 321 (1980).
[30] R. J. Lombard and D. Mas, private communication in Ref. [33].
[31] C. Pomar, J. Blomqvist, R. J. Liotta, and A. Insolia, Nucl. Phys. **A515**, 381 (1990).
[32] V. Gillet, B. Giraud, and M. Rho, J. Phys. (Paris) **37**, 189 (1976).
[33] C. N. Papanicolas, J. Heisenberg, J. Lichtenstadt, J. S. McCarthy, D. Goutte, J. M. Cavedon, B. Frois, M. Huet, P. Leconte, Phan Xuan Ho, and S. Platchkov, Phys. Rev. Lett. **52**, 247 (1984).
[34] V. R. Brown and V. A. Madsen, Phys. Rev. C **11**, 1298 (1975); **17**, 1943 (1978).
[35] V. R. Brown, A. M. Bernstein, and V. A. Madsen, Phys. Lett. **164B**, 217 (1985).
[36] V. A. Madsen and V. R. Brown, Phys. Rev. C **38**, 1428 (1988).
[37] A. M. Bernstein, V. R. Brown, and V. A. Madsen, Comments Nucl. Part. Phys. **11**, 203 (1983).